2021 43rd Annual International Conference of the
IEEE Engineering in Medicine & Biology Society (EMBC)
Oct 31 - Nov 4, 2021. Virtual Conference

Dimensionality Reduction of Local Field Potential Features with Convolution Neural Network in Neural Decoding: A Pilot Study

Xingchen Ran, Yiwei Zhang, Chenye Shen, Blaise Yvert, Weidong Chen, Shaomin Zhang*

***Abstract*—Local field potentials (LFPs) have better long-term stability compared with spikes in brain-machine interfaces (BMIs). Many studies have shown promising results of LFP decoding, but the high-dimensional feature of LFP still hurdle the development of the BMIs to low-cost. In this paper, we proposed a framework of a 1D convolution neural network (CNN) to reduce the dimensionality of the LFP features. For evaluating the performance of this architecture, the reduced LFP features were decoded to cursor position (Center-out task) by a Kalman filter. The Principal components analysis (PCA) was also performed as a comparison. The results showed that the CNN model could reduce the dimensionality of LFP features to a smaller size without significant performance loss. The decoding result based on the CNN features outperformed that based on the PCA features. Moreover, the reduced features by CNN also showed robustness across different sessions. These results demonstrated that the LFP features reduced by the CNN model achieved low cost without sacrificing high-performance and robustness, suggesting that this method could be used for portable BMI systems in the future.**

I. Introduction

The brain-machine interfaces (BMIs) have developed rapidly in recent years, especially towards speech decoding [1, 2] or computer cursor / robotic arm control [3-5]. By using the electroencephalogram (EEG) or electrocorticography (ECoG) grid or Microelectrode array to record neural activities, the BMI decoders can directly translate the intention of users into the control commands of external devices [6-8]. Although lots of promising progress have been achieved recently, the performance of BMI is still limited by recording methods and characteristics of the neural signals. Normally, the recorded neural activities have attributes like high-dimensional and strong-relevant inputs, low signal-to-noise ratio, poor long-term stability [10], etc. These attributes heavily affect BMI decoders both on computing time and decoding performance.

The neural signal binning and decoding rates have a significant impact on a real-time BMI system [11]. Common BMI decoding algorithms at present like Kalman filter (KF) [6] or optimal linear estimation (OLE) [9] need to calculate the inverse of the matrix in each step of the prediction, which brings a huge computation burden when processing high-dimensional neural data such as local frequency potential (LFP) or multi-array spikes, especially of the non-PC, portable devices like FPGAs or DSPs. Dethier et al. [12] reported that the power consumption of an x86 processor was 1.8mW approximately to perform 2D Kalman filtering on a 96-channel array. Moreover, the consumption of time and power dramatically rises with the increase of neural features. In addition, Weiss et al. [13] developed a portable BMI system by integrating a wearable neural signal processor hub (wNSP hub) with a medical-grade tablet PC. Their system demonstrated that running decoding tasks on relatively low-performance tablet hardware may result in poor performance, manifested by irregular timing and poor battery life. In general, to address the power-consuming problem, one option is to choose more powerful hardware, which might mean a trade-off between portability and performance. Another option is to develop novel decoding algorithms to reduce power consumption [12, 14]. And the last option is to utilize the redundancy between neural activities to reduce the feature number, which aims to employ the fewer neural features to maintain the optimum decoding performance.

In this study, we proposed a framework of a 1D convolution neural network (CNN) to reduce the dimensionality of the LFP features when offline analyzing these LFP signals collected from the primary cortex (M1) of one monkey during a center-out task. The performance of our CNN method was compared with classical Principal components analysis (PCA). Our results show: 1) The CNN-based dimensionality reduction features achieved significantly higher daily decoding performance than PCA-based features; 2) The CNN model could compress LFP features to lower dimensions than PCA without degrading the decoding performance; 3) The CNN model trained in the former session can be applied to the following sessions without significant decoding performance loss.

II. Data and Methodology

A. Data Acquisition

In this study, a monkey had a silicon 96-electrode microelectrode array (Blackrock Microsystems) implanted in the left M1, contralateral to the right arm used to control the cursor. The microelectrode array was implanted in the arm area, as estimated visually from local anatomical landmarks. All surgeries and experimental protocols were approved by the Guide for The Care and Use of Laboratory Animals (China

*This research supported by the National Key R&D Program (2017YFE0195500) and the NSFC (31627802, 31371001), the Key R&D Program of Zhejiang (2021C03003, 2021C03050).

Xingchen Ran, Yiwei Zhang is with Qiushi Academy for Advanced Studies, Department of Biomedical Engineering, Zhejiang University, Hangzhou, China.

Chenye Shen are with the Department of Biomedical Engineering and Instrument Science, Zhejiang University, Hangzhou, China.

Blaise Yvert is with Inserm and University Grenoble Alpes, BrainTech Lab U1205, Grenoble, France.

Weidong Chen and Shaomin Zhang* is with Qiushi Academy for Advanced Studies of Zhejiang University, Key Laboratory of Biomedical Engineering of Ministry of Education, Zhejiang Provincial Key Laboratory of Cardio-Cerebral Vascular Detection Technology and Medicinal Effectiveness Appraisal, Hangzhou, Zhejiang, China. (corresponding author, phone: +86 571 87952838; fax: +86 571 87952865; e-mail: shaomin@zju.edu.cn).

Ministry of Health) and the Animal Care Committee at Zhejiang University, China.

The 96-channel neural data from M1 were recorded by the Cerebus aquization system (Blackrock Microsystems) at a sample rate of 2000Hz. The behavioral data were recorded by a joystick which is connected to a computer with USB (sampled at 100Hz) and is down-sampled to 10Hz for analysis. LFP signals were band-pass filtered from 0.3 Hz to 400 Hz. Different frequency bands of 0.3-5 Hz, 5-8 Hz, 8-13 Hz, 13-30Hz, 70-200 Hz, 200-400 Hz were extracted separately. And the extracted LFP spectral power was furtherly down-sampled to 10 Hz and aligned with behavioral data. In this study, five sessions across five days were recruited. The average recording time was 40.75 minutes (652 trials) in each session.

B. CNN-based Dimensionality Reduction Model

The object of dimensionality reduction of LFP features includes reducing the number of electrodes n, and the number of frequency bands m. From the perspective of reducing network size, the network reducing m frequency bands then n channels have fewer parameters than of the network directly reducing $m \times n$ LFP matrix. Besides, the network that reduces m and n separately may be more interpretable than the direct reduction network.

The main module of the CNN model is a 1D convolutional layer with kernel size 1×1 followed by an instance normalization layer [15] and leaky rectified linear activation (LReLU) [16]. 1×1 convolution is widely used in dimensionality reduction to reduce the network parameters [17, 18], which is one of the main reasons why we chose this approach. Moreover, 1×1 convolution exchanged information between channels by linearly combining different weighted signal sequences. And the non-linear characteristics of these linear feature combinations have been increased via the involvement of the leaky ReLU activation function. The architecture of the CNN model is shown in Fig. 1, with details listed in Table I.

The network aims to minimize the mean square error between the actual cursor position and the prediction position decoded from the reduced LFP features by optimizing the following loss function:

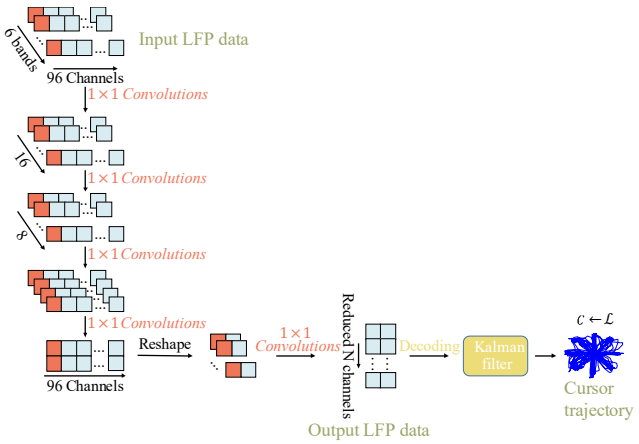

Fig. 1. Dimensionality reduction model architecture. The input LFP data first go through 4 1×1 convolution layers to reduce the number of frequency bands to 2, then transpose the output and input it to another 1×1convolution layer to reduce the number of electrodes. The reduced LFP features decoded by Kalman filter to cursor position on the screen.

TABLE I. CNN PARAMETERS

Input: LFP (6 × 96)
Conv1D (16), IN, LReLU, width=1, stride=1
Conv1D (8), IN, LReLU, width =1, stride=1
Conv1D (4), IN, LReLU, width =1, stride=1
Conv1D (2), IN, LReLU, width =1, stride=1
Transpose: (96 × 2)
Conv1D (*N*), width =1, stride=1
Output: dimension reduced LFP (*N* ×2)

$$\mathcal{L} = \frac{1}{2}\mathrm{E}([\Phi(\mathrm{C}(z)) - y]^2) \qquad (1)$$

Where Φ represents the neural-to-kinematic mapping function, C is the CNN dimensionality reduction network, z is the recorded LFP data, and y is the actual cursor positions.

In this network, a Kalman Filter (KF) was used as the Φ function to constrain the learning of C during training epochs. The training and prediction of KF followed the method in [19]. In each step of the training phase, $\mathrm{C}(z)$ is randomly divided into two consecutive parts f_1 and f_2. f_1 is used to estimate the state and measurement parameters of the Kalman filter. And f_2 is used to predict cursor position. The update of parameters of C only depends on f_2, as f_1 used to train Kalman filter has no contribution to the loss computation.

C. PCA-based Dimensionality Reduction

The PCA-based dimensionality reduction method was employed as a control of our CNN-based dimensionality reduction in this study. Different from that the CNN model reduces the number of frequency bands and electrodes separately, the PCA method directly cuts down the number of LFP features [20]:

$$\mathrm{P}\Delta Q^T = \mathrm{svd}(\mathrm{z} - \bar{z}) \qquad (2)$$

$$z_{reduced} = zQ_n \qquad (3)$$

Where Q denotes the coefficients of the linear combinations of z, n is the size of the target dimension.

For comparing the dimensionality reduction results between CNN and PCA, the output of the two methods was fed into the Kalman filter to predict cursor position during the testing. The correlation coefficient (CC) and mean square error (MSE) were used as the metrics to evaluate their performance.

III. EXPERIMENTS AND RESULTS

A. Model Training

The CNN model parameters used are listed in Table I. "LN" denotes the instance normalization, and Conv1D (*N*) denotes a one-dimensional convolution layer with *N* channels. The weights and bias of each convolution layer were initialized by normal distribution $\mathcal{N}(0, 0.02)$ and constant 0, respectively. This model was trained by Adam optimizer [21] with max epoch 100, and the initial learning rate was set to 0.001. The early stopping rule was utilized to prevent over-fitting. When the validation loss did not decrease in 7 epochs, the training was terminated. The model was implemented using Pytorch with CUDA.

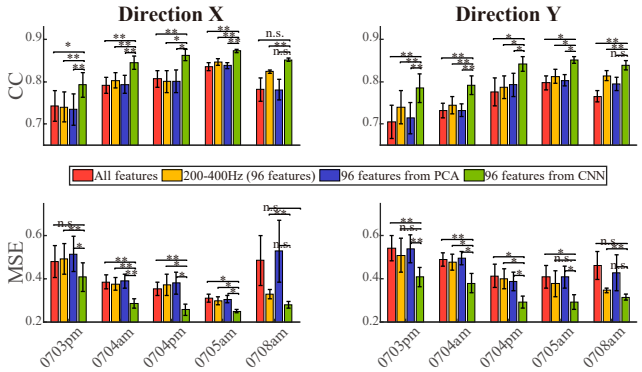

Fig. 2. Decoding results of Kalman filter of 4 different types of features. All LFP features (96 channels with 6 frequency bands, red bar), only 200-400 Hz features (96 channels, yellow bar), and PCA-based dimensionality reduced LFP features (blue bar) are used to compare with CNN based dimensionality reduced features (green bar). The stars denote the CNN-based features significantly outperformed other methods (paired t-test).

B. *Decoding Accuracy of the Reduced LFP Data*

The reduced dimension was set to 96 features, which averagely explained 90.48% variance in PCA overall five sessions data. And that means we reduced the $N = 48$ in our CNN model. A five-fold cross-validation was used to investigate the decoding consistency. The dataset in each session was split into 0.4, 0.4, and 0.2 as the training dataset, validation dataset, and test dataset. After dimensionality reduction, the processed features from the PCA-based method and CNN-based method were decoded to the cursor position by the Kalman filter. As a comparison for the dimensionality reduction effect, we also decoded all frequency bands (576) and just 200-400 Hz of LFP that was found more relevant to the movement [22]. The decoding results showed that the features from our CNN significantly outperformed (paired t-test, $p < 0.05$) the features from PCA in the first four sessions in both directions, but not the last session. This caused by the last session recording software paused several times in the beginning, made the recording unstable in the first fold. Moreover, the decoding results of the CNN reduced features also significantly outperformed all features decoding and only 200-400 Hz decoding (paired t-test, $p < 0.05$). The decoding results showed in Fig. 2. 100 seconds example of decoding trajectory from CNN-based features (green line) and PCA-based features (blue line) showed in Fig. 3. The green line fits the actual trajectory well, while the blue line had some error predicted peak values , suggesting that the CNN-based features generate a more accurate neural-to-kinematic mapping.

C. *The Decoding Performance of Different Number of Components*

The above results showed the high performance of the CNN model when the number of dimensions reduced to 96, it is suggested that the dimension of the LFP signal may still have potential redundancy. To explore the minimum dimensionality that can maintain the high decoding performance, we set the N to 2, 8, 16, 32, 48, 64, and 80 while the corresponding PCA components are 4, 16, 32, 64, 96, 128, and 160 respectively. Fig. 4 showed that compared to the 96 LFP features, the average decoding CC and MSE of 4 LFP features obtained from CNN only decreased by 1.64% and -8.59%, respectively. However, for 4 LFP features from PCA,

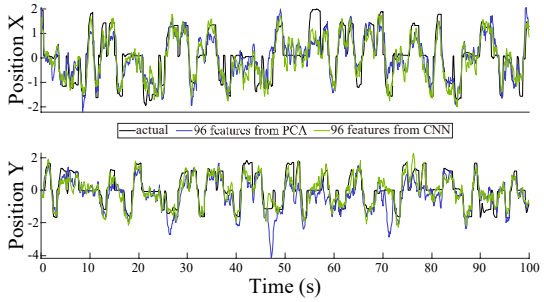

Fig. 3. Decoded trajectory example of dimensionality reduced by PCA and CNN.

the average decoding CC and MSE decreased by 57.94% and -158.49%, respectively.

IV. Discussion

In this study, we demonstrated that a network architecture consisting of five 1×1 convolution layers was able to reduce the dimension of LFP features. A neural-to-kinematic mapping function was introduced to regularize the training of our model. Furthermore, our proposed CNN model maintained high-performance decoding with features of small number components, significantly outperformed the PCA features with same number of components.

A. *Relationship between the decoding costs and the dimensionality of LFP*

The Kalman filter process has two steps: (1) the state $\hat{x}_{t+1}$ prediction using the state equation and the current state x_t, and (2) the update of the predicted state $\hat{x}_{t+1}$ based on the measurements z_{t+1}. The computational cost of updating the Kalman filter is $O(nm^2 + n^2m)$ [23], where n is the dimension of x, m is the dimension of z. For BMI application, especially for LFP based BMI, if $m \gg n$, makes the consumption of time and power dramatically rises with the increase of m. Research has shown that running spikes with 96 electrodes to a 2-degree Kalman filter on an x86 processor took 0.985us/update, consumes 1.82mW for 20 updates/sec [13, 24]. This lack of low-power decoding hinders the development of the BMI. However, our results showed our CNN model could reduce the dimension of LFP features from 576 to 4, and maintain high-performance decoding. When

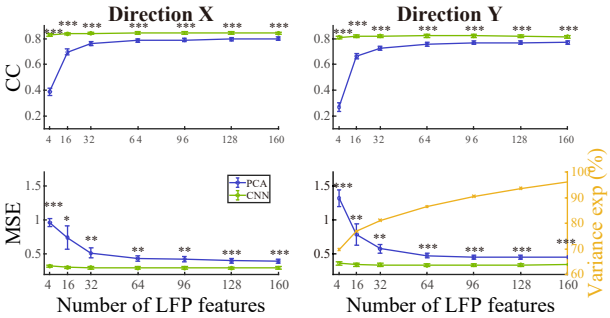

Fig. 4. Decoding results of different dimensionality. The stars denote decoding results of CNN features significantly outperformed PCA features (paired t-test). The yellow line is the variance explanation of PCA of the different numbers of features.

reducing the dimension of LFP signals to 4, the time costs of our CNN model and Kalman filter are $O(96 \times 268) + O(48) = O(25776)$, which is much lower than the costs of decoding LFP directly ($O(2 \times 576^2 + 2^2 \times 576)$). It suggests that our CNN model can reduce the power costs and speed up the decoding process dozens of times.

C. Interpretability of the CNN model

Our CNN model reduces the number of frequency bands and the number of electrodes sequentially, when reducing the number of frequency bands, the number of electrodes remains constant, vice versa. Reducing the dimension of frequency bands can be treated as a weighted linear combination of different frequencies, then non-linearity is added by the activation function. These reduced bands might be higher-order representations of brain states [25]. Reducing the number of electrodes also a process of weighted linear combination of different electrodes, but no activation function is applied. Moreover, by reducing the number of frequencies first, the size of the network is smaller compared to reduce the number of electrodes first. This makes 30 minutes of data is sufficient to train our CNN model.

However, in this pilot study, we only demonstrated the CNN model performance by decoding. The analysis of the reduced LFP features is insufficient. Our work at the next step may focus on analyzing the properties of the reduced LFP features to get a better understanding of the network and the LFP signals.

V. Conclusions

This paper proposed a dimensionality reduction method using five layers of a 1D 1×1 convolution neural network to reduce the frequency bands and electrodes separately. Using the Kalman filter as the decoder, the decoding accuracy of the reduced features from our method outperforms the non-reduced LFP features and those extracted by PCA. Moreover, the CNN model can compress the dimension of LFP signals to a smaller size without significant performance loss. Compared to the 96 reduced features, four reduced features from CNN has a performance loss of 1.64%, while the PCA has a performance loss of 57.94%.

References

[1] Anumanchipalli, G. K., Chartier, J., & Chang, E. F. (2019). Speech synthesis from neural decoding of spoken sentences. *Nature, 568*(7753), 493-498.

[2] Akbari, H., Khalighinejad, B., Herrero, J. L., Mehta, A. D, & Mesgarani, N. (2019). Towards reconstructing intelligible speech from the human auditory cortex. *Scientific Reports, 9*(1).

[3] Flesher, S. N., Collinger, J. L., Foldes, S. T., Weiss, J. M., Downey, J. E., & Tyler-Kabara, E. C, et al. (2016). Intracortical microstimulation of human somatosensory cortex. *Science Translational Medicine, 8*(361), 361ra141.

[4] Pandarinath, C., Nuyujukian, P., Blabe, C. H., Sorice, B. L., Saab, J., Willett, F. R., ... & Henderson, J. M. (2017). High performance communication by people with paralysis using an intracortical brain-computer interface. *Elife*, *6*, e18554.

[5] Gilja, V., Pandarinath, C., Blabe, C. H., Nuyujukian, P., Simeral, J. D., Sarma, A. A., ... & Henderson, J. M. (2015). Clinical translation of a high-performance neural prosthesis. *Nature medicine*, *21*(10), 1142.

[6] Hochberg, L. R., Serruya, M. D., Friehs, G. M., Mukand, J. A., Saleh, M., Caplan, A. H., ... & Donoghue, J. P. (2006). Neuronal ensemble control of prosthetic devices by a human with tetraplegia. *Nature*, *442*(7099), 164-171.

[7] Velliste, M., Perel, S., Spalding, M. C., Whitford, A. S., & Schwartz, A. B. (2008). Cortical control of a prosthetic arm for self-feeding. *Nature*, *453*(7198), 1098-1101.

[8] Santhanam, G., Ryu, S. I., Byron, M. Y., Afshar, A., & Shenoy, K. V. (2006). A high-performance brain–computer interface. *nature*, *442*(7099), 195-198.

[9] Wodlinger, B., Downey, J. E., Tyler-Kabara, E. C., Schwartz, A. B., Boninger, M. L., & Collinger, J. L. (2014). Ten-dimensional anthropomorphic arm control in a human brain-machine interface: difficulties, solutions, and limitations. *Journal of neural engineering*, *12*(1), 016011.

[10] Sussillo, D., Stavisky, S. D., Kao, J. C., Ryu, S. I., & Shenoy, K. V. (2016). Making brain–machine interfaces robust to future neural variability. *Nature communications*, *7*(1), 1-13.

[11] Cunningham, J. P., Nuyujukian, P., Gilja, V., Chestek, C. A., Ryu, S. I., & Shenoy, K. V. (2011). A closed-loop human simulator for investigating the role of feedback control in brain-machine interfaces. *Journal of neurophysiology*, *105*(4), 1932-1949.

[12] Dethier, J., Nuyujukian, P., Ryu, S. I., Shenoy, K. V., & Boahen, K. (2013). Design and validation of a real-time spiking-neural-network decoder for brain–machine interfaces. *Journal of neural engineering*, *10*(3), 036008.

[13] Weiss, J. M., Gaunt, R. A., Franklin, R., Boninger, M. L., & Collinger, J. L. (2019). Demonstration of a portable intracortical brain-computer interface. *Brain-Computer Interfaces*, *6*(4), 106-117.

[14] Boi, F., Moraitis, T., De Feo, V., Diotalevi, F., Bartolozzi, C., Indiveri, G., & Vato, A. (2016). A bidirectional brain-machine interface featuring a neuromorphic hardware decoder. *Frontiers in neuroscience*, *10*, 563.

[15] Ulyanov, D., Vedaldi, A., & Lempitsky, V. (2016). Instance normalization: The missing ingredient for fast stylization. *arXiv preprint arXiv:1607.08022*.

[16] Xu, B., Wang, N., Chen, T., & Li, M. (2015). Empirical evaluation of rectified activations in convolutional network. *arXiv preprint arXiv:1505.00853*.

[17] Szegedy, C., Liu, W., Jia, Y., Sermanet, P., Reed, S., Anguelov, D., ... & Rabinovich, A. (2015). Going deeper with convolutions. In *Proceedings of the IEEE conference on computer vision and pattern recognition* (pp. 1-9).

[18] He, K., Zhang, X., Ren, S., & Sun, J. (2016). Deep residual learning for image recognition. In *Proceedings of the IEEE conference on computer vision and pattern recognition* (pp. 770-778).

[19] Wu W, Black M J, Gao Y, et al. Inferring Hand Motion from Multi-Cell Recordings in Motor Cortex using a Kalman Filter. 2002.

[20] Abdi, H., & Williams, L. J. (2010). Principal component analysis. *Wiley interdisciplinary reviews: computational statistics*, *2*(4), 433-459.

[21] Kingma, D. P., & Ba, J. (2014). Adam: A method for stochastic optimization. *arXiv preprint arXiv:1412.6980*.

[22] Rickert, J., de Oliveira, S. C., Vaadia, E., Aertsen, A., Rotter, S., & Mehring, C. (2005). Encoding of movement direction in different frequency ranges of motor cortical local field potentials. *Journal of Neuroscience*, *25*(39), 8815-8824.

[23] Paz, L. M., Tardós, J. D., & Neira, J. (2008). Divide and conquer: EKF SLAM in $ o (n) $. *IEEE Transactions on Robotics*, *24*(5), 1107-1120.

[24] Dethier, J., Gilja, V., Nuyujukian, P., Elassaad, S. A., Shenoy, K. V., & Boahen, K. (2011, April). Spiking neural network decoder for brain-machine interfaces. In *2011 5th International IEEE/EMBS Conference on Neural Engineering* (pp. 396-399). IEEE.

[25] Tort, A. B., Kramer, M. A., Thorn, C., Gibson, D. J., Kubota, Y., Graybiel, A. M., & Kopell, N. J. (2008). Dynamic cross-frequency couplings of local field potential oscillations in rat striatum and hippocampus during performance of a T-maze task. *Proceedings of the National Academy of Sciences*, *105*(51), 20517-20522.